

values of the corresponding direct-excitation cross sections. The uncertainties associated with the absolute cross sections listed in Tables I and II are relative to the experimental measurements of this paper only. They do not take into account possible uncertainties in the data of Ref. 9, which were used to place our relative measurements on an absolute scale.

The relative values of the  $4^3S$  and  $3^3P$  direct-excitation cross sections are plotted on a log-log scale as a function of electron-impact energy (Fig. 4). The error bars represent the limits of experimental reproducibility and take into account measurement errors present in each of the quantities used to determine the direct cross section. A weighted least-squares analysis of the data indicates that the  $4^3S$  direct cross section de-

creases with increasing electron energy according to the relation  $(\text{energy})^{-2.8 \pm 0.2}$ , while the  $3^3P$  cross section decreases as  $(\text{energy})^{-3.0 \pm 0.2}$ . In each case the rate of decrease exhibits reasonable agreement with the dc intensity measurements of Kay and Showalter.<sup>4</sup>

It appears that above electron energies of 50 eV both the  $4^3S$  and  $3^3P$  direct cross sections follow an  $(\text{energy})^{-3}$  dependence. This result would appear to contradict the  $(\text{energy})^{-2}$  dependence predicted by Born-Oppenheimer theory for the  $4^3S$  level, and instead tends to support the expansion technique of Ochkur and Bratsev. The present work demonstrates the versatility and promise of time-resolved spectroscopy as a research tool when used in conjunction with absolute-intensity measurements.

\*Supported in part by the National Science Foundation.

<sup>1</sup>N. F. Mott and H. S. W. Massey, *The Theory of Atomic Collisions*, 3rd ed. (Clarendon, Oxford, England, 1965).

<sup>2</sup>V. I. Ochkur and V. F. Bratsev, *Opt. Spektrosk.* **19**, 490 (1965) [*Opt. Spectrosc.* **19**, 274 (1965)].

<sup>3</sup>B. L. Moisewitsch and S. J. Smith, *Rev. Mod. Phys.* **40**, 246 (1968).

<sup>4</sup>R. B. Kay and J. G. Showalter, *Phys. Rev. A* **3**, 1998 (1971).

<sup>5</sup>R. J. Anderson, R. H. Hughes, and T. G. Norton, *Phys. Rev.* **181**, 198 (1969).

<sup>6</sup>R. J. Anderson and R. H. Hughes, *Phys. Rev. A* **5**, 1194 (1972).

<sup>7</sup>R. H. Hughes, R. B. Kay, and L. D. Weaver, *Phys. Rev.* **129**, 1630 (1963).

<sup>8</sup>A. H. Gabriel and D. W. O. Heddle, *Proc. R. Soc. Lond.* **A258**, 124 (1960).

<sup>9</sup>R. M. St. John, F. L. Miller, and C. C. Lin, *Phys. Rev.* **134**, A888 (1964).

<sup>10</sup>W. R. Pendleton and R. H. Hughes, *Phys. Rev.* **138**, A683 (1965).

## Time and Pressure Dependence of the Vacuum-Ultraviolet Radiation in Neon

Peter K. Leichner

*Department of Physics and Astronomy, University of Kentucky, Lexington, Kentucky 40506*

(Received 6 March 1973)

A 250-keV electron accelerator was used to carry out time-dependent studies in neon gas at the wavelength of the  $^1P_1$  and  $^3P_1$  resonance line and the 850-Å continuum over a wide range of pressures, up to 1000 Torr. The resonance line decays exponentially with a lifetime that is governed predominantly by the escape of resonance radiation to the walls of the emission chamber and by three-body destruction of the resonance states. The main continuum near 859 Å comes to a maximum well after termination of the excitation pulse and then decays with a lifetime that is very long at low pressures. However, this lifetime decreases with increasing pressure at low and intermediate pressures and assumes a nearly constant value of 5.1 μsec at the highest pressures. From the time-dependent studies it is proposed that both  $^1P_1$  and  $^3P_1$  resonance states are converted to metastable molecular states by three-body collisions. The metastable molecules in turn may undergo two- and three-body collisions with ground-state atoms which convert them to radiative molecules that radiate the 850-Å continuum with a lifetime of about 5.1 μsec.

### I. INTRODUCTION

Recent investigations of the vacuum-ultraviolet (vuv) radiation in argon<sup>1</sup> and helium<sup>2</sup> have shown that the excitation of noble gases by energetic charged particles provides a valuable tool for

measuring the time and pressure dependence of the resonance radiation and continuous emission in these gases. The objective of this paper is to report lifetime measurements of the 740-Å resonance line and the 850-Å continuum in pure neon gas over wide pressure ranges.

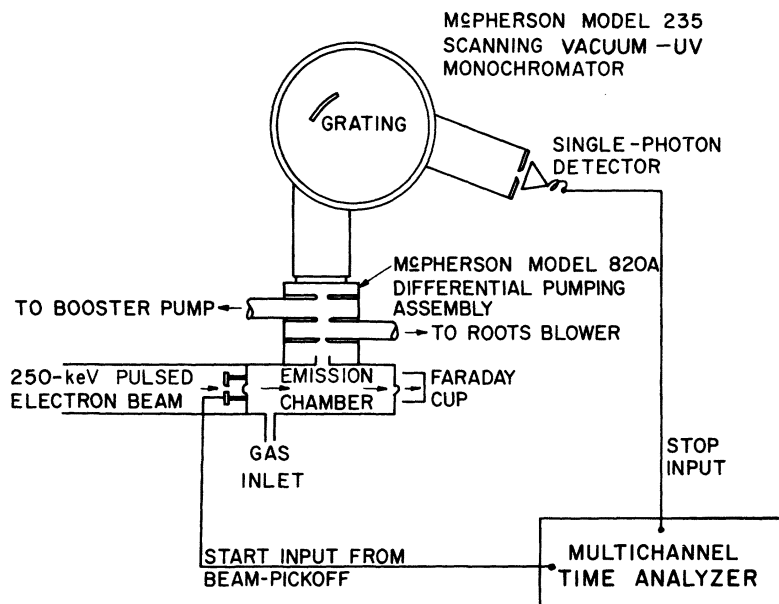


FIG. 1. Schematic diagram of apparatus for measuring vuv emissions as a function of pressure, time, and wavelength.

Lifetime data provide important information on the depletion of resonance states as a function of pressure, the pressure dependence of the vuv continua, and the kinetic rates associated with the energy pathways that lead to the continuous emissions. Thus, results of lifetime measurements are of significant value in assigning atomic precursors to the observed continua in the noble gases. It is emphasized, however, that lifetime measurements alone do not lead to unique models. In addition to the time-dependent studies reported in Refs. 1 and 2 and in this work, important experimental input data are provided by measurements in the pure noble gases of the  $W$  values<sup>3</sup> (absorbed energy per ion pair), the intensity of the vuv emissions as a function of wavelength and pressure,<sup>4,5</sup> the fraction of energy lost by the charged particles that goes into light emission,<sup>6</sup> as well as the increase in ionization (Jesse effect) resulting from the addition of impurities,<sup>3</sup> and the quenching of light owing to these impurities.<sup>7</sup>

By utilizing the results of the above investigations in conjunction with other experimental and theoretical work, one eventually hopes to find a unifying model for a given radiation-matter system.

## II. EXPERIMENTAL METHOD

A detailed description of the electron accelerator and associated electronics has been given elsewhere<sup>1,8</sup>; therefore we confine our remarks to the experimental technique, represented schematically in Fig. 1, that was used to make lifetime measurements in neon. Pulsed 250-keV

electrons enter a cylindrical stainless-steel emission chamber through a 0.000 03-in.-thick nickel foil, interact with the neon gas while traveling along the axis of the chamber, and exit through a second nickel foil, 0.0001 in. thick. The electrons are then collected in a Faraday cup. The emitted photons enter a scanning vuv monochromator, are reflected by a diffraction grating, and are detected using single-photon counting techniques.

The intensity of the vuv radiation as a function of wavelength and pressure was observed by scanning the monochromator through the wavelengths of interest for each pressure  $P$ . Time-dependent measurements were made by a time-of-flight technique. Before entering the emission chamber, some of the electrons from the leading edge of the pulse strike a beam pickoff and generate a synchronization signal that starts the time scan of the multichannel analyzer. The detected photons stop the time scan, and the time dependence of

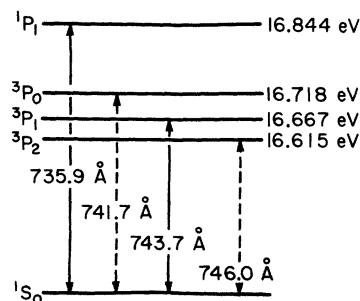


FIG. 2. Energy-level diagram for neon showing the first few excited states.

the emissions is determined for each wavelength over wide ranges of pressure.

As the resonance radiation and continuous emission in neon occur in the 700–1000-Å range, the gas had to be differentially pumped to keep the monochromator evacuated. Gas pressure in the emission chamber ranged from 25 to 1000 Torr, whereas the pressure in the monochromator never exceeded  $10^{-5}$  Torr. A good grade of neon (ultra-high-purity Linde gas) was used with an assayed purity of 99.995%. Gas purity was maintained by using stainless-steel gas lines, an ultrahigh-purity pressure reducer, and a reluctance manometer for pressure determination. Before taking data, the emission chamber was evacuated to a pressure of less than  $10^{-6}$  Torr for at least 48 h.

The resolution of the monochromator was 8 Å at full width at half-maximum (FWHM) with the monochromator entrance and exit slits used.

### III. RESULTS

Figure 2 shows a term level diagram of the first few excited states of the neon atom.<sup>9</sup> The  $^3P_2$  and  $^3P_0$  states are metastable because of selection rules forbidding electric dipole radiation to the ground state. The  $^1P_1$  state, on the other hand, radiates to the ground state by an allowed dipole radiation. The  $^3P_1$  state radiates to the ground state because of the mixing of the singlet and triplet wave functions due to the lack of pure Russell-Saunders coupling.<sup>10</sup>

Typical neon spectra as a function of wavelength and pressure are displayed in Fig. 3. These spectra are characterized by a fairly sharp resonance line in the 740-Å region and a broad continuum in the 850-Å region, centered at about 830 Å. At intermediate pressure (less than 300 Torr) a second weak continuum is observed in the 1000-Å region; for pressures up to 50 Torr it was possible to observe both the 744- and 736-Å resonance lines; the latter could not be resolved at the higher pressures. A representative low-pressure spectrum is given by the upper diagram in Fig. 3. These observations are in full agreement with the proton-induced spectra reported by Stewart *et al.*,<sup>4</sup> who also suggest that the two continua may have different atomic precursors or are produced by different kinetic processes. Both the electron- and proton-induced spectra differ from the less reproducible gas-discharge work.<sup>4–11</sup> Figure 4 displays typical time-dependent studies for the resonance line. The peak intensity shifts to slightly longer wavelengths at higher pressure, an effect that was also observed in argon<sup>1</sup>; Hurst *et al.*<sup>12</sup> suggested absorption by van der Waals molecules as an explanation for this. As it was desir-

able to follow the peak intensity during the course of the experiment in order to maintain reasonable count rates, data were taken at 250 Torr for different wavelengths within the resonance line to ascertain whether the wavelength shift affected the lifetime measurements; however, no wavelength dependence was observed. Table I lists the decay parameters of the resonance line obtained from computer fitting the data to the equation

$$I_1(t) = a_1 e^{-u_1 t} + a_2 e^{-u_2 t}. \quad (1)$$

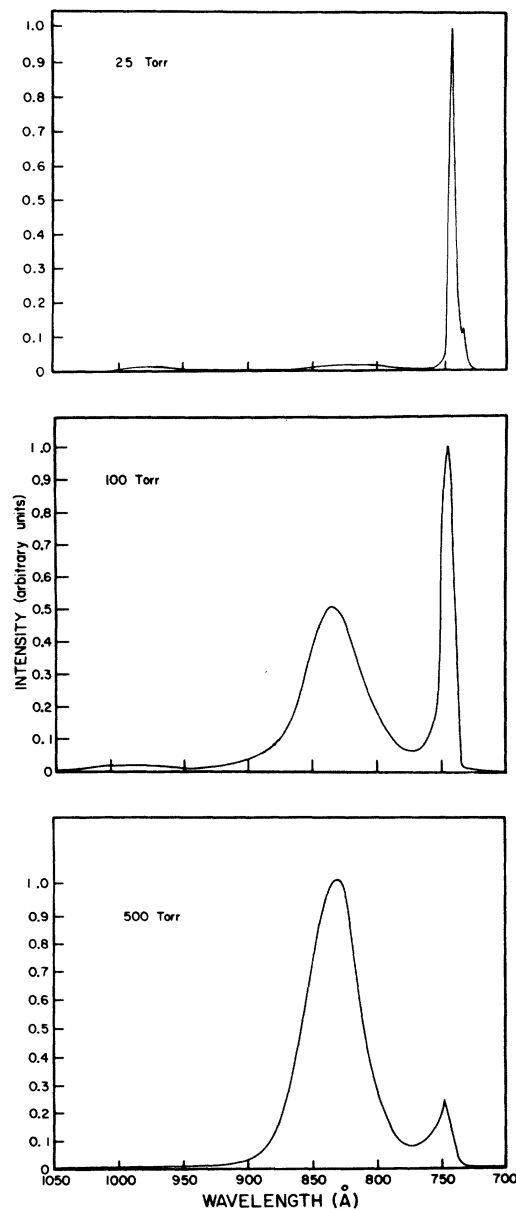


FIG. 3. Neon spectra in the vuv region as a function of pressure and wavelength.

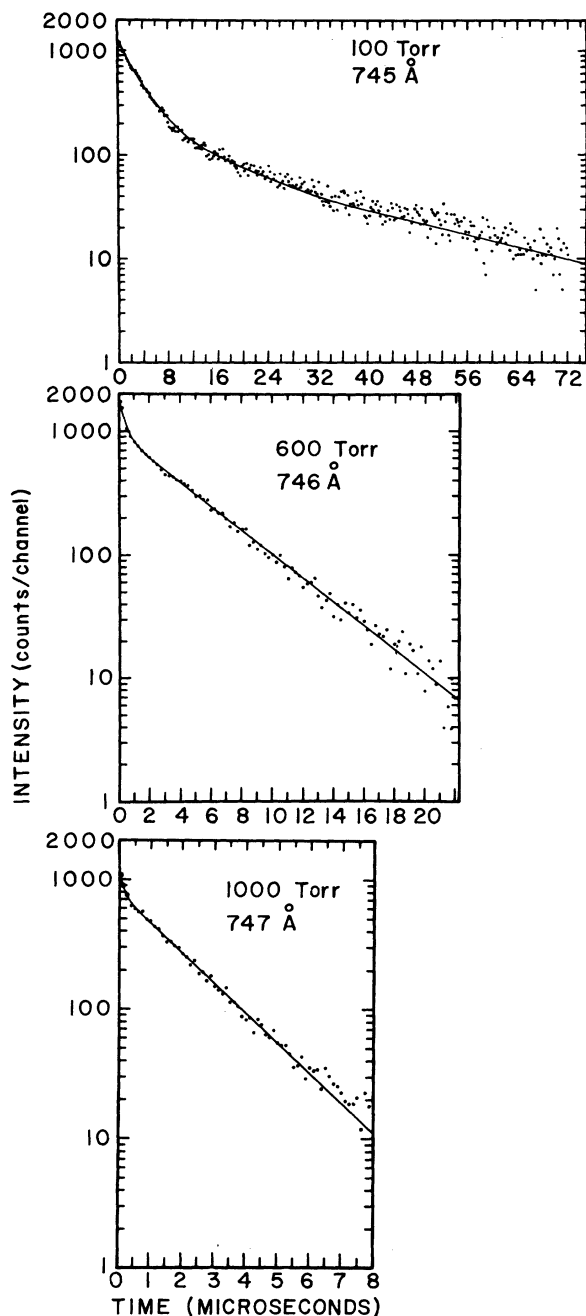


FIG. 4. Typical time-resolved spectra of the 740-Å resonance line. The solid line was obtained by computer fitting the data to Eq. (1).

Both the fast ( $u_1$ ) and the slow ( $u_2$ ) decay constants were quite reproducible, and it is estimated that the error in them is about 5%. The time dependence of the resonance line can be interpreted in terms of Holstein's<sup>13,14</sup> theory of resonance photon trapping and by three-body collision processes. The decay to trapped resonance photons is des-

cribed by an exponential expression of the form

$$I(t) = N_0 e^{-\beta t}, \quad (2)$$

where  $\beta$  is Holstein's<sup>14</sup> pressure-independent decay constant given by

$$\beta = \frac{0.2069}{\tau} \left( \frac{\lambda}{R} \right)^{1/2}. \quad (3)$$

The quantity  $\tau$  is the natural lifetime of the resonance state,  $\lambda$  is the corresponding wavelength, and  $R$  is the radius, equal to 2.22 cm, of the cylindrical emission chamber. Lawrence and Liszt<sup>15</sup> have measured the natural lifetimes of the  $^1P_1$  and  $^3P_1$  states to be  $1.87 \pm 0.18$  and  $31.7 \pm 1.6$  nsec, respectively. Using these values, one obtains from Eq. (3)

$$\beta_1 = 0.2014 \times 10^6 \text{ sec}^{-1} \quad (4)$$

for the  $^1P_1$  state and

$$\beta_2 = 0.01194 \times 10^6 \text{ sec}^{-1} \quad (5)$$

for the  $^3P_1$  state. If three-body collisions are proposed to transfer energy out of these states, the experimental decay constants should satisfy expressions of the form

$$u_a = \beta_1 + c_1 P^2 \quad (^1P_1), \quad (6)$$

$$u'_a = \beta_2 + c_2 P^2 \quad (^3P_1), \quad (7)$$

where  $P$  is the pressure in Torr. With  $c_1 = 7.29 \pm 0.35 \text{ sec}^{-1}/\text{Torr}^2$  and  $c_2 = 0.562 \pm 0.03 \text{ sec}^{-1}/\text{Torr}^2$ , the above equations fit the data quite well, as shown in Fig. 5. The agreement suggests that the observed fast decays arise entirely from the  $^1P_1$  state, whereas the slow decay components are due to the  $^3P_1$  state; both states decay with lifetimes that appear to be governed predominantly by the escape of resonance radiation to the walls of the emission chamber and by a three-body depletion mechanism. We also note that the experimental decay constants continue to increase as the pressure increases, so that the above values of  $\beta_1$  and  $\beta_2$  are lower limits.

The time dependence of the 850-Å continuum (see Fig. 6) displays an interesting feature also observed in argon<sup>1</sup>; the intensity of the radiation continues to increase after termination of the beam pulse. Maximum intensity was reached approximately 30  $\mu\text{sec}$  at 50 Torr and 2.5  $\mu\text{sec}$  at 1000 Torr after the excitation pulse was terminated. The widths of the excitation pulses are given in Table II. The buildup and decay of the 850-Å continuum was computer fitted to the difference of two exponentials:

TABLE I. Decay constants for the  $^1P_1$  and  $^3P_1$  time dependence [obtained by fitting Eq. (1) to data].

Pressure (Torr)	$\lambda$ (Å)	Pulse width ( $10^{-4}$ sec)	$a_1$	$a_2$	$u_1$ ( $10^6$ sec $^{-1}$ )	$u_2$ ( $10^6$ sec $^{-1}$ )
25	744	1.0	2105	162	0.1171	0.007870
50	744	0.5	2380	167	0.1438	0.01150
100	745	0.5	1740	120	0.3063	0.02428
150	745	0.5	2310	156	0.4378	0.03459
200	745	0.5	3530	234	0.5955	0.04849
250	745	0.5	6190	394	0.7789	0.05929
300	746	0.5	9950	675	1.088	0.08490
400	746	0.5	6810	421	1.409	0.1315
600	746	0.5	18900	1160	2.992	0.2392
800	747	0.5	28100	1740	4.862	0.3683
1000	747	0.5	20050	1235	6.985	0.5469

$$I_2(t) = -a_3 e^{-u_3 t} + a_4 e^{-u_4 t}. \quad (8)$$

Table II summarizes the quantities  $u_3$  and  $u_4$  corresponding to the rise and decay, respectively, of the continuum radiation.

A model to account for the time evolution of the 850-Å continuum is discussed in the next section.

#### IV. MODEL FOR 850-Å CONTINUUM

In this section an energy-pathways model is proposed to account for the time evolution of the 850-Å continuum, consistent with the decay of the 740-Å resonance line. The construction of this model is facilitated by previous work, particu-

larly as regards the argon model.<sup>1</sup>

The time-independent spectra (Fig. 3) show that in neon there is one main continuum which increases strongly in intensity with pressure. The corresponding decrease in intensity of the resonance line suggests that the richly populated  $^1P_1$

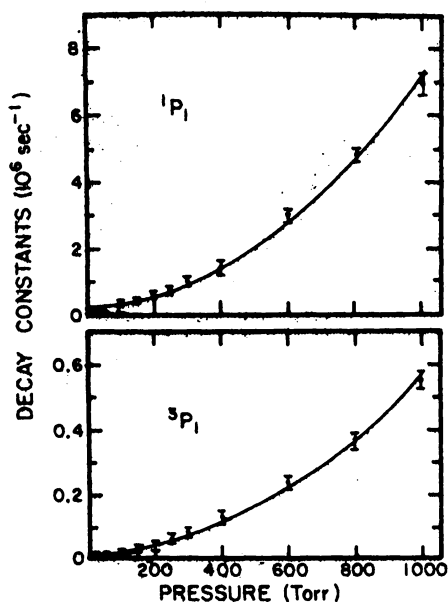


FIG. 5. Pressure dependence of the  $^1P_1$  (upper diagram) and  $^3P_1$  (lower diagram) decay constants. The solid lines were calculated from Eqs. (6) and (7). The data points are tabulated in Table I, where  $u_1$  and  $u_2$  correspond to the  $^1P_1$  and  $^3P_1$  decay constants, respectively.

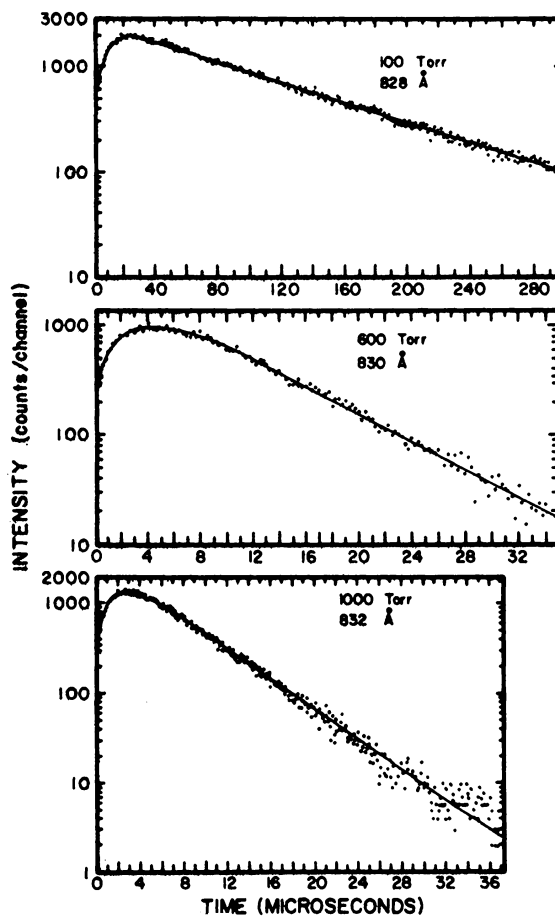


FIG. 6. Typical time-resolved spectra of the 850-Å continuum. The solid line was obtained by computer fitting the data to Eq. (8).

TABLE II. Calculated parameters for the 850-Å time dependence [obtained by fitting Eq. (8) to data].

Pressure (Torr)	$\lambda$ (Å)	Pulse width ( $10^{-8}$ sec)	$-a_3$	$a_4$	$u_3$ ( $10^8$ sec $^{-1}$ )	$u_4$ ( $10^8$ sec $^{-1}$ )
50	828	1.0	646	1050	0.076 64	0.005 734
100	828	1.0	2603	3047	0.082 87	0.011 89
150	828	0.5	1797	2000	0.1073	0.023 27
200	829	0.5	1672	1915	0.1091	0.032 30
250	830	0.5	5766	5989	0.1235	0.053 93
300	830	0.5	2604	2875	0.1362	0.054 90
600	831	0.5	2794	3017	0.3216	0.1415
800	831	0.5	2976	3159	0.3840	0.1829
1000	832	0.5	3377	3587	0.3973	0.1967

and  $^3P_1$  states, which should lead to emission in some form, may be primarily responsible for the continuous emission. Furthermore, from the time-dependent studies (Figs. 4 and 6) it is seen that the decay of the resonance states occurs within the rise time of the continuum and that the decrease in time lag for the continuum at higher pressures correlates with the shorter lifetime of the resonance states at these pressures. Thus, the data indicate qualitatively that the 850-Å continuum may indeed originate from the resonance states. A more quantitative discussion is given below.

The  $P^2$  terms in the depletion of the resonance states (Fig. 5) may be interpreted to mean that metastable neon molecules are formed when excited atoms are depleted by three-body collisions with ground-state atoms. The data in Table II show that the decay constant  $u_4$  increases with pressure at low and intermediate pressures but assumes a nearly constant value at the highest pressures. This also suggests that metastable molecules are formed which store energy until collisions convert them to radiative molecules; the high-pressure value of  $u_4$  implies that the 850-Å continuum represents an allowed transition in the neon molecule.

Figure 7 shows the energy-pathways model based on the above ideas. In this model, the three-body depletion rate of the resonance states follows directly from the 740-Å data [Eqs. (6) and (7)]; the rate of decay of the radiative molecule is the 1000-Torr value of  $u_4$  corresponding to a molecular lifetime of about 5.1  $\mu$ sec. The only adjustable parameter—namely, the two- and three-body collision rates at which metastable molecules are converted to radiative ones—was obtained by computer fitting the time-dependent 850-Å data to the model. The following quantities are defined:  $N_1(t)$  is the number of neon atoms in the  $^1P_1$  state,  $N_2(t)$  is the number of neon molecules in the metastable  $(Ne)_2^M$  state, and  $N_3(t)$  is the number of neon molecules in the radiating

$(Ne)_2^R$  state. The quantity  $c_1P^2$  is the rate of destruction of  $^1P_1$  states by three-body collisions, and  $b_1P + b_2P^2$  is equal to the rate of conversion of metastable molecules to radiative ones by two- and three-body collisions. The rate of decay of radiative molecules by spontaneous emission is denoted by  $u$ . One then has the following rate equations:

$$\frac{dN_1(t)}{dt} = -u_a N_1(t), \quad (9)$$

$$\frac{dN_2(t)}{dt} = c_1 P^2 N_1(t) - (b_1 P + b_2 P^2) N_2(t), \quad (10)$$

$$\frac{dN_3(t)}{dt} = (b_1 P + b_2 P^2) N_2(t) - u N_3(t), \quad (11)$$

with

$$N_1(t) = N_0 e^{-u_a t}. \quad (12)$$

This leads to

$$N_3(t) = C \left( \frac{e^{-u_b t}}{u - u_b} - \frac{e^{-u_a t}}{u - u_a} + \frac{(u_a - u_b) e^{-u t}}{(u - u_a)(u - u_b)} \right), \quad (13)$$

where

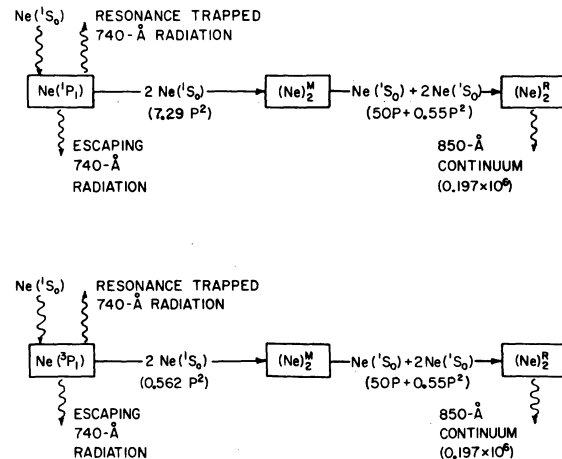


FIG. 7. Model for the 850-Å continuous emission in neon. The numbers in parentheses are in units of sec $^{-1}$ .

$$C = c_1 P^2 u_b N_0 / (u_a - u_b), \quad (14)$$

and where  $N_0$  is the initial number of  $^1P_1$  states. Using similar definitions for the  $^3P_1$  states, one finds their contribution to the continuous emission to be given by

$$N'_3(t) = C' \left( \frac{e^{-u_b t}}{u - u_b} - \frac{e^{-u'_a t}}{u - u'_a} + \frac{(u'_a - u_b) e^{-u t}}{(u - u'_a)(u - u_b)} \right), \quad (15)$$

with

$$C' = c_2 P^2 u_b N'_0 / (u'_a - u_b), \quad (16)$$

$$u_b = b_1 P + b_2 P^2, \quad (17)$$

and where  $N'_0$  is the initial number of  $^3P_1$  states. The time evolution of the continuum is then described by

$$N(t) = N_3(t) + N'_3(t). \quad (18)$$

The time evolution of Eq. (18) was computed for neon gas pressures ranging from 50 to 1000 Torr. The ratio of  $^1P_1$  to  $^3P_1$  states at each pressure was obtained directly from the 740-Å data; that is, the ratio of the coefficients  $a_1$  to  $a_2$  taken from Table I was used as the ratio of  $^1P_1$  to  $^3P_1$  states in calculating the time evolution of the continuum. Numerical values of the two- and three-body collision terms, which appear in Eq. (17), were obtained by normalization to the continuum data at 100 and 1000 Torr. With these values Eq. (17) becomes

$$u_b = 50P + 0.55P^2. \quad (19)$$

Calculations of the time profile, based on Eqs. (18) and (19), agree with the data quite well over the entire range of pressures and are as good as the computer fits shown in Fig. 6.

Over the range of pressures 50–1000 Torr the ratio of  $^1P_1$  to  $^3P_1$  states varies from about 14.2 to 16.6, in reasonable agreement with the ratio of oscillator strengths of the  $^1P_1$  to  $^3P_1$  levels (Lawrence and Liszt<sup>15</sup> report a value of about 17). The slightly lower ratios at the lower pressures may be due to collisional excitation and deexcitation of the metastables to the nearest radiating ( $^3P_1$ ) state. Neon gas-discharge studies<sup>16,17</sup> have shown that these effects are particularly important at low and intermediate pressures. As a result of the imprisonment of resonance radiation, one must also consider the possibility of collisional conversion of atoms in the radiating states to metastable ones; however, it appears that for the range of pressures and the very early times under consideration in our analysis, atoms in the radiating states are predominantly destroyed by three-body collisions. The early times are of particular importance to this

work because most of the energy that escapes from the resonance states appears at the early times.

The work of Phelps<sup>16</sup> shows that atoms in the  $^3P_2$  metastable state are also destroyed by three-body collisions involving two ground-state atoms at a rate equal to  $0.626P^2$ . To determine whether this state contributes significantly to the 850-Å radiation in neon, a  $^3P_2$  channel was admitted to the model in place of the  $^3P_1$  channel shown in Fig. 7. The alternative model thus included the  $^1P_1$  channel and allowed for a  $^3P_2$  channel, very similar to the model previously used for argon<sup>1</sup>; that is, a conversion of  $^3P_2$  atoms to radiating  $(\text{Ne})_2^R$  molecules via three-body collisions at a rate of  $0.626P^2$ . Computer calculations based on the alternative model did not give good agreement with experiment. It appears that in neon the continuum radiation arises predominantly from the  $^1P_1$  and  $^3P_1$  states, although a small contribution from the  $^3P_2$  level should not be ruled out completely.

## V. DISCUSSION

From the analysis of experimental data in the preceding sections, it was suggested that the radiating  $^1P_1$  and  $^3P_1$  states in neon are destroyed primarily by the escape of resonance radiation to the walls of the container and by three-body collisions involving two ground-state atoms. Gas-discharge studies<sup>16</sup> of the decay of  $^3P_1$  atoms do not report a three-body destruction rate for them. However, this does not contradict the findings reported here, because the gas-discharge data were analyzed late in the afterglow, whereas the analysis presented here refers to the very early times. The gas-discharge work<sup>16</sup> does, in fact, show that  $^3P_1$  atoms are destroyed much more rapidly at early than at late times in the afterglow.

The three-body collision rates determined in Sec. III were used to construct an energy-pathways model to explain the origin of the 850-Å continuum radiation. The model suggests that the  $^1P_1$  and  $^3P_1$  atoms give rise to the same radiating neon molecule. This is consistent with the symmetry of the continuum. A more definitive test was made by measuring the time dependence of the vuv emission at a constant pressure of 250 Torr at various wavelengths within the continuum. No wavelength dependence was found. This may mean that indeed only one type of molecule is involved in the continuum radiation. The fact that the decay of the 850-Å continuum assumes a nearly constant value at the highest pressures was interpreted to mean that the radiative molecule has a lifetime of approximately  $5.1 \mu\text{sec}$ . There appears to be no other experimental evidence on the lifetime of the

radiative neon molecule.

#### ACKNOWLEDGMENTS

The author is grateful to G. S. Hurst, G. Payne, N. Thonnard, and R. E. Knight for interesting and

helpful discussions. Particular thanks are due to G. S. Hurst and G. Payne for reading the manuscript. Numerical calculations were carried out using facilities of the University of Kentucky Computing Center.

<sup>1</sup>N. Thonnard and G. S. Hurst, *Phys. Rev. A* **5**, 1110 (1972).

<sup>2</sup>D. M. Bartell, Ph.D. thesis (University of Kentucky, 1972) (unpublished).

<sup>3</sup>J. E. Parks, Ph.D. thesis (University of Kentucky, 1970) (unpublished).

<sup>4</sup>T. E. Stewart, G. S. Hurst, T. E. Bortner, J. E. Parks, F. W. Martin, and H. L. Weidner, *J. Opt. Soc. Am.* **60**, 1290 (1970).

<sup>5</sup>T. E. Stewart, Ph.D. thesis (University of Kentucky, 1970) (unpublished).

<sup>6</sup>G. S. Hurst, T. E. Stewart, and J. E. Parks, *Phys. Rev. A* **2**, 1717 (1970).

<sup>7</sup>H. L. Weidner, University of Kentucky (unpublished).

<sup>8</sup>N. Thonnard, Ph.D. thesis (University of Kentucky, 1971) (unpublished).

<sup>9</sup>The energy levels are taken from C. E. Moore, *Atomic Energy Levels*, Natl. Bur. Stds. Circ. No. 467 (U. S. GPO, Washington, D.C., 1949), Vol. 1, p. 77.

<sup>10</sup>G. H. Shortley, *Phys. Rev.* **47**, 295 (1935).

<sup>11</sup>Y. Tanaka, A. S. Jursa, and F. J. LeBlanc, *J. Opt. Soc. Am.* **48**, 304 (1958).

<sup>12</sup>G. S. Hurst, T. E. Bortner, and T. D. Strickler, *Phys. Rev.* **178**, 4 (1969).

<sup>13</sup>T. Holstein, *Phys. Rev.* **72**, 1212 (1947).

<sup>14</sup>T. Holstein, *Phys. Rev.* **83**, 1159 (1951).

<sup>15</sup>G. M. Lawrence and H. S. Liszt, *Phys. Rev.* **178**, 122 (1969).

<sup>16</sup>A. V. Phelps, *Phys. Rev.* **114**, 1011 (1959).

<sup>17</sup>E. E. Wisniewski, J. T. Verdeyen, and B. E. Cherrington, *Bull. Am. Phys. Soc.* **16**, 206 (1971).

## Formulation of the Binary-Encounter Approximation in Configuration Space and Its Application to Ionization by Light Ions\*

J. S. Hansen

*Cyclotron Institute, Texas A&M University, College Station, Texas 77843*

(Received 20 February 1973)

The binary-encounter approximation (BEA) is transformed from momentum space to configuration space. In this frame the impact-parameter representation allows one to calculate a variety of quantities pertinent to the general problem of ionization. Among these are cross sections for proton ionization of hydrogen and helium; in the latter case, cross sections for ejection of both electrons are also given. A number of tables and formulas are given, enabling one to correct the simple hydrogenlike-model predictions of the BEA for effects which arise in multielectron atoms. Multiple-ionization probabilities ( $K + L$  shell) are calculated and compared to experimental results and to the predictions of the semiclassical approximation.

### I. INTRODUCTION

A vast amount of literature over the past several years has been devoted to experimental and theoretical inquiries into the effects which arise when a charged particle passes through an atomic charge cloud. With increased enthusiasm and ingenuity, researchers have obtained experimental results which refute many of the simplest predictions of the prevailing theories. Although many of these theoretical failures may arise because of the often concomitant alteration of the atom and hence its resemblance with the simple model by which it may be theoretically described, these same failures have created an environment stimulating to

the theoretical reinvestigation of some of the details of charged-particle atomic collisions.

The present paper is presented with two distinct objectives in mind. The first goal is one of formulating in configuration space a model of the interaction of two charged particles, a bound electron and a particle of fixed trajectory with respect to the nucleus. The model evolves from a transformation of the widely used binary-encounter approximation (BEA) from momentum space into configuration space and then through a reexpression in the impact-parameter representation. The latter representation enables one to view the interaction process in terms of *probabilities* from which the cross sections can be obtained.